



Constrained spheroids for prolonged hepatocyte culture



Wen Hao Tong^{a, b, c}, Yu Fang^{a, b, c}, Jie Yan^{a, c, g}, Xin Hong^c, Nisha Hari Singh^a,
Shu Rui Wang^d, Bramasta Nugraha^{a, b, e, f}, Lei Xia^c, Eliza Li Shan Fong^c,
Ciprian Iliescu^{a, **}, Hanry Yu^{a, b, c, g, h, i, *}

^a Institute of Biotechnology and Nanotechnology, A*STAR, The Nanos, #04-01, 31 Biopolis Way, Singapore 138669, Singapore

^b NUS Graduate School for Integrative Sciences and Engineering, Centre for Life Sciences (CeLS), #05-01, 28 Medical Drive, Singapore 117456, Singapore

^c Department of Physiology, Yong Loo Lin School of Medicine, MD9-03-03, 2 Medical Drive, Singapore 117597, Singapore

^d Bruker Singapore Pte Ltd., 11 Biopolis Way #10-10, The Helios, Singapore 138667, Singapore

^e ETH Zürich, Department of Biosystem Science and Engineering (D-BSSE), Mattenstrasse 26, CH-4058 Basel, Switzerland

^f Roche Pharmaceutical Research and Early Development, Department of Discovery Technology, Roche Innovation Center Basel, Grenzacherstrasse 124, CH-4070 Basel, Switzerland

^g Singapore-MIT Alliance for Research and Technology, 1 CREATE Way, #10-01 CREATE Tower, Singapore 138602, Singapore

^h Mechanobiology Institute, National University of Singapore, T-Lab, #05-01, 5A Engineering Drive 1, Singapore 117411, Singapore

ⁱ Department of Biological Engineering, Massachusetts Institute of Technology, Cambridge, MA 02139, USA

ARTICLE INFO

Article history:

Received 11 November 2015

Accepted 29 November 2015

Available online 3 December 2015

Keywords:

Hepatocytes

Spheroids

Liver

Perfusion

Drug testing

ABSTRACT

Liver-specific functions in primary hepatocytes can be maintained over extended duration *in vitro* using spheroid culture. However, the undesired loss of cells over time is still a major unaddressed problem, which consequently generates large variations in downstream assays such as drug screening. In static culture, the turbulence generated by medium change can cause spheroids to detach from the culture substrate. Under perfusion, the momentum generated by Stokes force similarly results in spheroid detachment. To overcome this problem, we developed a Constrained Spheroids (CS) culture system that immobilizes spheroids between a glass coverslip and an ultra-thin porous Parylene C membrane, both surface-modified with poly(ethylene glycol) and galactose ligands for optimum spheroid formation and maintenance. In this configuration, cell loss was minimized even when perfusion was introduced. When compared to the standard collagen sandwich model, hepatocytes cultured as CS under perfusion exhibited significantly enhanced hepatocyte functions such as urea secretion, and CYP1A1 and CYP3A2 metabolic activity. We propose the use of the CS culture as an improved culture platform to current hepatocyte spheroid-based culture systems.

© 2015 Elsevier Ltd. All rights reserved.

1. Introduction

In vitro liver models enable rapid evaluation of drug bioavailability and hepatotoxicity, both of which are critical measures in the drug development process [1]. Among the various *in vitro* models developed to mimic drug metabolism *in vivo*, such as cultured liver slices [2], microsomes [3], and cell lines [4,5], primary hepatocytes remain the most relevant and practical model as they possess the necessary Phase I and Phase II metabolizing enzymes, xenosensors,

and transporter expression while maintaining acceptable throughput capacity [6]. However, primary hepatocytes rapidly lose their histotypic architecture, polarity and liver-specific functions when cultured on conventional tissue culture plastic [7,8]. To circumvent this problem, the collagen sandwich culture was developed; hepatocytes cultured between two layers of gelled collagen matrix retain key functions such as urea and albumin synthesis, Cytochrome (CYP) P450 enzyme activities, cortical F-actin cytoskeleton distribution and polarity over longer periods of time [9,10]. Still, the collagen sandwich culture has its limitations, including the use of collagen which exhibits batch-to-batch variation [11] and instability over time [12] in culture, as well as the barrier effect of the top collagen layer to drug access [13].

An alternative to the collagen sandwich model is the hepatocyte spheroid model where hepatocytes have been reported to retain

* Corresponding author. Department of Physiology, Yong Loo Lin School of Medicine, MD9-03-03, 2 Medical Drive, Singapore 117597, Singapore.

** Corresponding author.

E-mail addresses: ciliescu@ibn.a-star.edu.sg (C. Iliescu), hanry_yu@nuhs.edu.sg (H. Yu).

in vivo-like structural polarity and form functional bile canaliculi [14]. When grown as spheroids, hepatocytes better maintain key liver-specific functions such as albumin production, urea synthesis, CYP P450 and glucuronidation activity [15–17] for extended durations as compared to the collagen monolayer culture [18,19] and collagen sandwich culture [20–22], likely due to the restoration of three-dimensional (3D) cytoarchitecture, and more *in vivo*-like cell–matrix and cell–cell interactions [23]. Various methods have been developed to generate 3D aggregates, such as the use of the hanging drop method [24], rotational bioreactors [25], micro-fabricated microwells [20,26], selectively-adhesive patterned structures [27], and liquid overlay method [28].

Despite the numerous advantages of growing hepatocytes as spheroids, these spheroid-based models are rarely used in drug screening due to the poor control over spheroid formation and retention during culture. For example, floating spheroids cultured in rotational culture systems, on non-adhesive surfaces [15] or ligand-modified films [29], have the tendency to merge with each other to form larger spheroids. This makes quantification and standardization of hepatocyte cell count challenging and therefore generates large, undesired deviations in downstream assays [23,30]. Moreover, the 3D architecture of spheroids also presents a barrier for the diffusion of nutrients, oxygen, drugs and metabolic waste, especially when spheroids reach the critical size limit [31]. While scaffolds such as polyurethane foams [32,33] and inverted colloidal crystal scaffolds [34] have been developed to limit spheroid size, the use of this approach is limited by potential drug adsorption onto the scaffold surface. Microfabricated substrates such as microwells [20,26] or ligand-link thin films [29] minimize the problem of drug adsorption but spheroids cultured in these platforms tend to detach from the surface during routine medium change. To increase the stability of spheroid attachment to surfaces, various approaches [29,35–38] aimed at promoting spheroid adhesion have been investigated, such as the conjugation of integrin-binding moieties [21,39–41]. However, such a method typically results in cell spreading and diminished hepatocyte function [42].

Another critical feature of the ideal hepatocyte spheroid model is the presence of fluid flow to improve mass transfer. Perfusion culture has been shown to improve the viability, life span and metabolic performance of primary hepatocytes [43] as a result of continuous nutrient supply and waste removal [23]. However, spheroids grown on low-adhesion or selectively-adhesive patterned substrates in perfusion culture are exposed to the momentum generated by Stokes force, which consequently results in spheroid detachment. Shear stress generated by fluid flow is also detrimental to hepatocyte function [44,45]. While the use of microspheres [46] or scaffolds [35] has been investigated as a means to protect hepatocytes from flow-induced shear stress, these systems typically do not address the other requirements of minimizing spheroid loss and drug adsorption.

To address the need for a hepatocyte culture system that minimizes spheroid loss during culture and enables the provision of perfusion, we asked if the mechanical immobilization of hepatocyte spheroids in a sandwich configuration would minimize cell loss while maintaining hepatic functions over time. To this end, we developed and characterized such a system, henceforth referred to as the Constrained Spheroids (CS) culture system. In this system, hepatocytes are first seeded on a low-adhesion substrate (glass coverslips modified with poly(ethylene glycol) (PEG) and galactose) to promote spontaneous spheroid formation. Following the formation of spheroids on the glass substrate, the spheroids are then immobilized with an overlay of a malleable, ultra-thin and porous membrane. We observed that this engineered CS culture configuration not only effectively minimizes cell loss during static culture,

but also during perfusion culture. We found that the provision of perfusion to the cultured hepatocyte spheroids enhances key liver-specific functions typically assessed during drug testing as compared to the same hepatocyte spheroids cultured under static conditions.

2. Materials and methods

2.1. Materials

10 mm diameter glass coverslips were purchased from Paul Marienfeld GmbH & Co. KG (Lauda-Königshofen, Germany). Silane-PEG-COOH, MW 5000 was purchased from Nanocs Inc. (New York, USA). The galactose ligand, 1-O-(6'-aminohexyl)-D-galactopyranoside (AHG, MW 279) was synthesized as described previously [29,47] and verified by NMR spectroscopy. Other chemicals were purchased from Sigma–Aldrich (Singapore) unless otherwise stated.

2.2. Fabrication of PET-PAA-AHG and glass-PEG-AHG (MW 5000)

Polyethylene terephthalate (PET) thin film was modified with polyacrylic acid (PAA) and the AHG galactose moiety was fabricated as previously described [39] to generate PET-PAA-AHG thin films. To fabricate Glass-PEG-AHG, 10 mm glass coverslips were cleaned with piranha solution at 120 °C for 30 min, rinsed with DI water and dried in 100% ethanol. PEG was conjugated onto the glass surface using Silane-PEG-COOH, MW 5000 (Nanocs Inc, USA) by submerging the cleaned glass coverslip in 2 mM Silane-PEG-COOH solution, freshly prepared with 95% ethanol, for 24 h. Conjugation of the AHG galactose moiety was achieved by first activating the PEG-COOH modified glass surface with 1-ethyl-3-(3-dimethylaminopropyl) carbodiimide (EDC) and N-hydroxysuccinimide (NHS) for 1 h and subsequently incubating the glass coverslip in 2 mg/mL AHG solution in 0.1 M phosphate buffer for 48 h. Both PET-PAA-AHG and Glass-PEG-AHG were sterilized with 70% ethanol for 2 h, followed by a rinse with sterile phosphate buffer saline.

2.3. Fabrication of Parylene C membrane and modification

The fabrication process of the Parylene C membrane is illustrated in Fig. 3A. 10.16 cm 300- μ m-thick silicon wafers, double polished, <100> crystallographic orientation, were cleaned in piranha solution ($\text{H}_2\text{SO}_4 \cdot \text{H}_2\text{O}_2$, 2:1) at 120 °C for 30 min. 2- μ m-thick silicon oxide was then grown on the silicon surface in a furnace (Tystar, US) by wet process at 1050 °C for 11 h. The silicon oxide layer was patterned to generate the mechanical anchor using the AZ7220 positive photoresist mask and a RIE process involving CHF_3/O_2 . The mechanical anchor was performed using a technology similar to the SCREAM process [48] in Deep RIE equipment (Alcatel 100 SE). Briefly, silicon was anisotropically etched using the conventional Bosch process to create straight trenches (4 μ m width, 30 μ m depth). This was followed by the Teflon passivation process (using C_4F_8 in the same Deep RIE system) to conformal coat the newly created trenches. The passivation layer was then anisotropically etched (top surface and bottom of the trench) maintaining the Teflon layer only on the sidewalls of the trenches (so that fresh silicon surface was exposed at the bottom of the trenches). The exposed silicon layer at the bottom was then anisotropically plasma etched using SF_6 chemistry in order to create a “mushroom-like” profile. Parylene C was deposited using a chemical vapour deposition process with the Specialty Coating System (Fig. 3A). This deposition method ensures a conformal deposition of the Parylene C layer in such a way that the “mushroom-like” trenches are

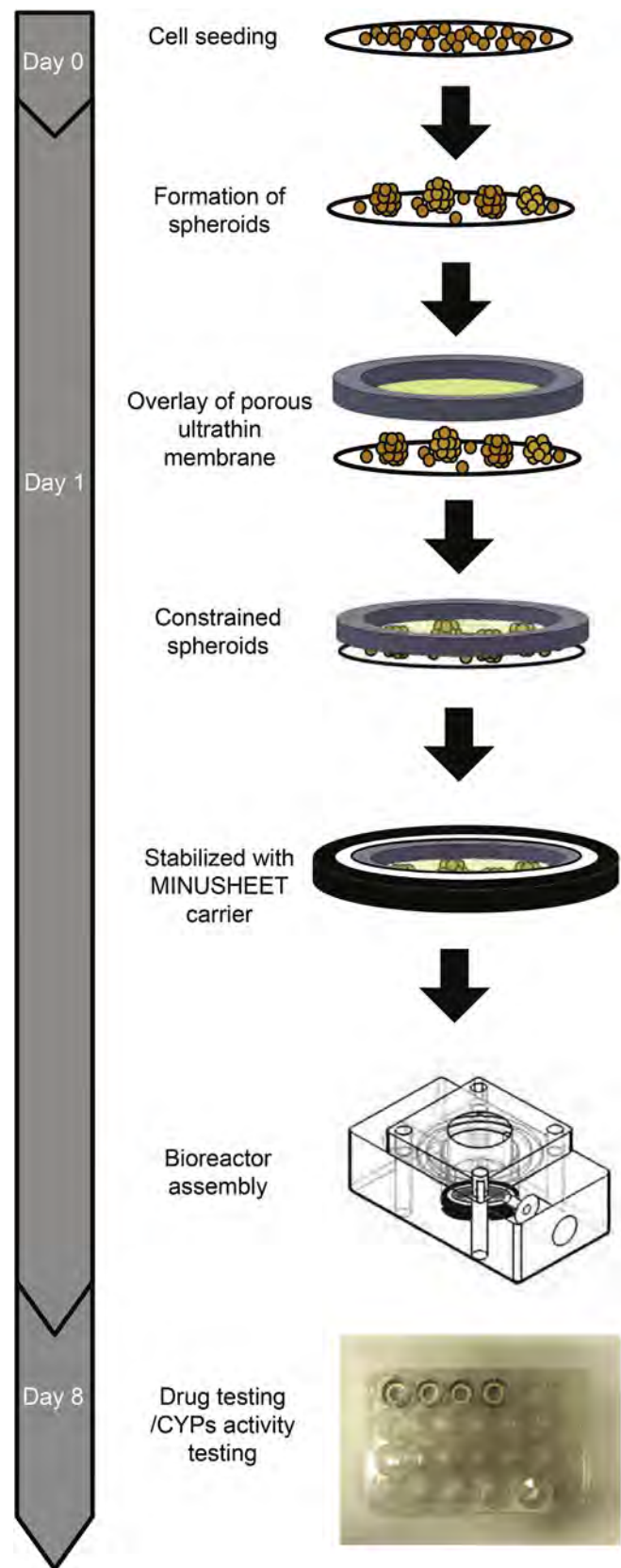


Fig. 1. Schematic of perfused constrained spheroids (CS) sandwich culture system set-up.

completely filled with Parylene C. The thickness of deposition was controlled by the amount of Parylene C monomers loaded into the system. The pores on Parylene C were then patterned using classical photolithographic and O_2 plasma etching processes, and the remaining photoresist layer was removed using NMP (Fig. 3A). A photoresist mask was applied on the back of the wafer. Through this photoresist mask, the silicon oxide layer was patterned in a similar manner as the mechanical anchor. Following which, the photoresist/ SiO_2 layer was used as a masking layer for the Bosch process in DRIE system to etch the silicon backbone, generating individual Parylene C membrane units from the silicon wafer. The etching process stopped once the silicon oxide layer (top surface) under the Parylene C membrane was fully etched. Finally the membranes were cleaned in NMP and residual silicon oxide was removed using BOE. A short annealing process on a hot plate ($110^\circ C$ for 10 min) provided tensile stress in the membrane, allowing the surface of the membrane to be perfectly flat.

The Parylene C membrane was modified according to a previously described method [48]. Briefly, the Parylene C membrane was oxidized by O_2 plasma (SAMCO PECVD BP-1) for 30 s, under 50 Pa and 125 W (RF power). The oxidized Parylene C membrane was then submerged in 2 mM Silane-PEG-COOH, MW 5000 in 95% ethanol for 24 h. The membrane was then washed with ethanol and PBS before activation with EDC and NHS for 1 h. 2 mg/mL AHG solution in 0.1 M phosphate buffer was then added to the membrane and incubated for 48 h. Modified Parylene C membrane was then sterilized in 70% ethanol for 2 h and rinsed with sterile PBS.

2.4. X-ray photoelectron spectroscopy (XPS) measurements

XPS was used to qualitatively verify the conjugation of PEG and galactose onto the glass coverslips. Measurements were made on a VG ESCALAB Mk II spectrometer with MgK α X-ray source (1253.6 eV photons) at a constant retard ratio of 40. High resolution spectra were collected for C and N elements.

2.5. Atomic force microscope (AFM) measurements

Experiments were conducted at room temperature with a Dimension Icon AFM system with a Nanoscope V controller and Nanoscope analysis (Bruker, Santa Barbara, CA). Nanomechanical measurements were performed using the PeakForce QNM (Quantitative NanoMechanics) mode which is based on the Derjaguin–Muller–Toropov (DMT) model on an AFM system under ambient conditions. Following calibration, samples were scanned using the ScanAsyst-air probe with a nominal radius of 2 nm and a nominal spring constant of 0.5 N m at a scan rate of 1 Hz.

Peak-force tapping AFM is an operating mode that can control the maximum normal force (“peak force”) applied on the samples at each point of the map. The force-separation curves collected were subsequently analysed to obtain information on sample adhesion, surface deformation and topography. Adhesion force is the minimum force depending on the interaction between the tip and sample while deformation is the difference of the separation from the force equal to zero to the peak force. The reduced elastic modulus E^* is obtained by fitting the experimental data using the Derjaguin–Muller–Toropov (DMT) model given by:

$$F_{tip} = \frac{4}{3}E^*(Rd^3)^{\frac{1}{2}} + F_{adh}$$

where F_{tip} is the force on the tip, F_{adh} is the constant adhesion force during contact, R is the tip end radius, and d is the tip to sample separation. The reduced modulus E^* is related to the sample elastic modulus E_s by:

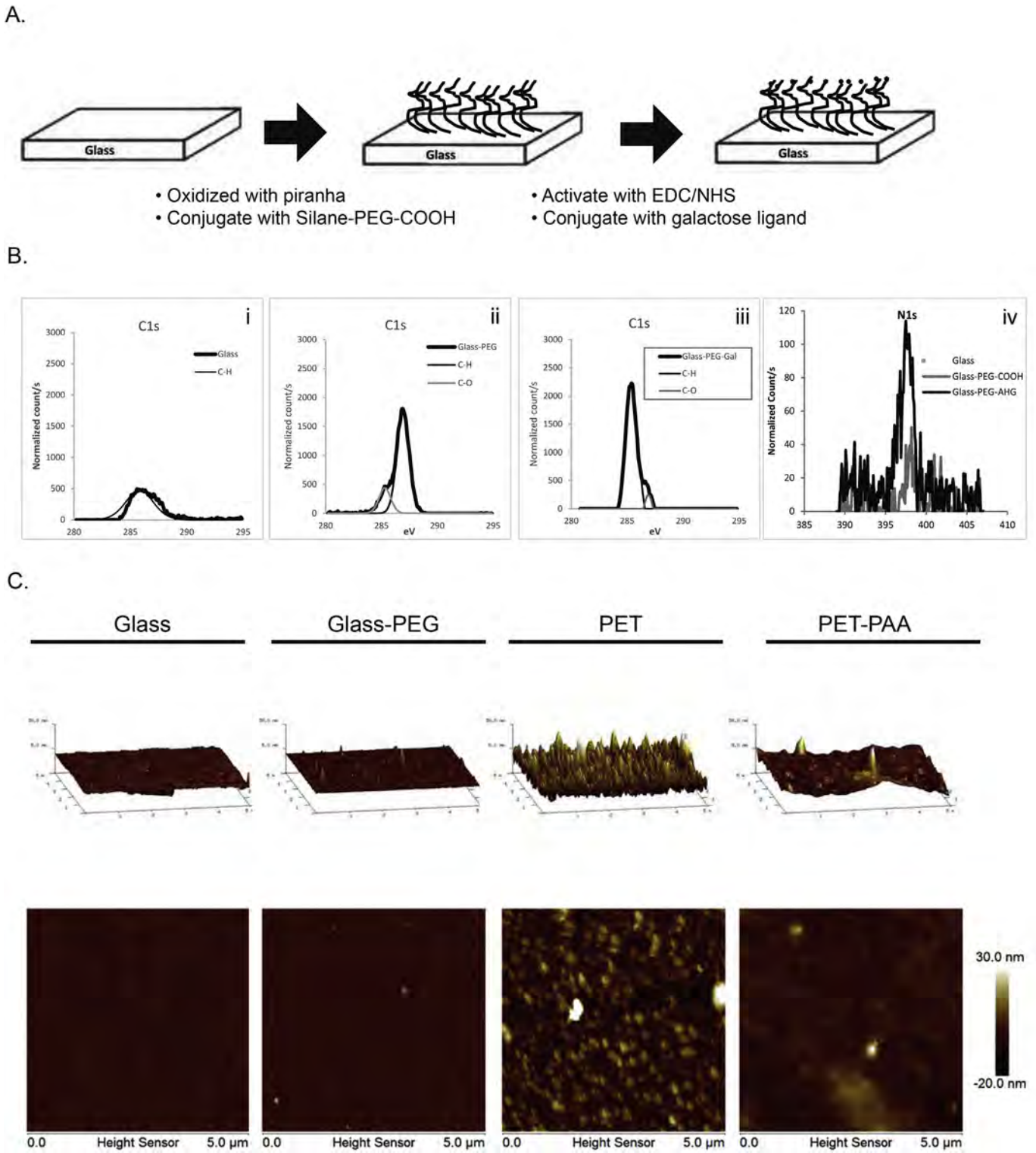


Fig. 2. Modification of bottom substrate to promote rapid hepatocyte spheroid formation. (A) Modification of glass coverslip with PEG and galactose moiety. (B) X-ray Photoelectron Spectroscopy (XPS) analysis of modified substrates, demonstrating the successful modification of glass coverslips with PEG and galactose moiety. (C) Atomic force microscopy images of Glass-PEG and PET-PAA substrates. (D) Brightfield time-lapse images of hepatocyte spheroids on Glass-PEG-AHG and PET-PAA-AHG substrates. Hepatocyte spheroids formed more quickly on Glass-PEG-AHG than PET-PAA-AHG. (E) Percentage of culture surface area covered by hepatocytes as a measure of spheroid formation.

$$E^* = \left[\frac{(1 - \nu_s^2)}{E_t} + \frac{(1 - \nu_s^2)}{E_s} \right]^{-1}$$

where ν and E are the Poisson's ratio and Young's modulus and the subscripts "t" and "s" stand for the tip and sample, respectively. In our system, the tip modulus, E_t , is much larger than E_s so that the first term of E^* equation above can be neglected. Hence, E_s is calculated easily given the Poisson's ratio ν_s .

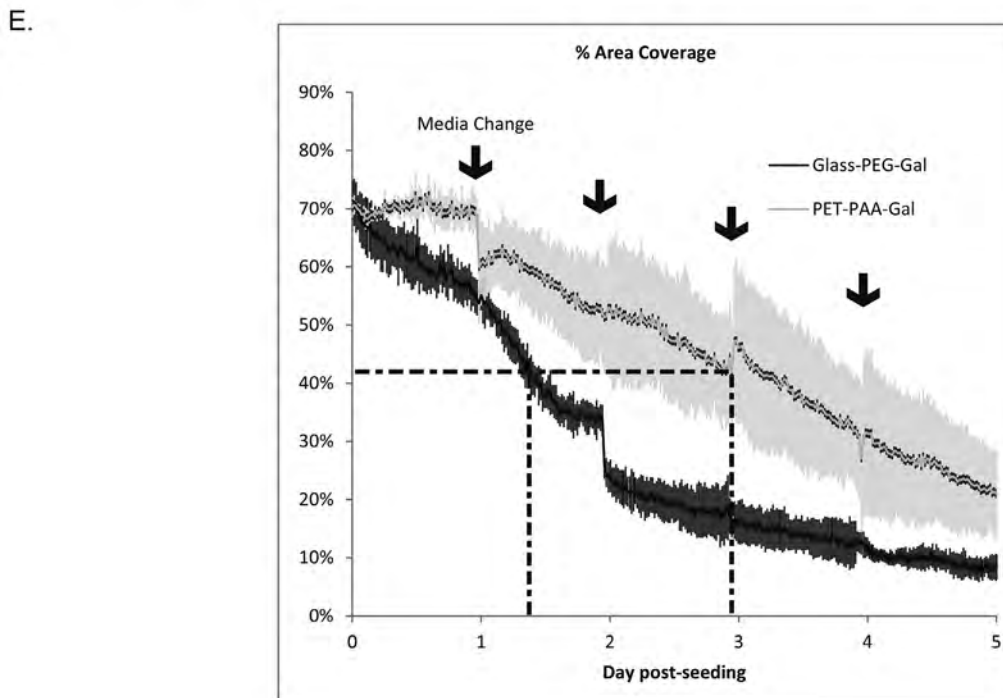
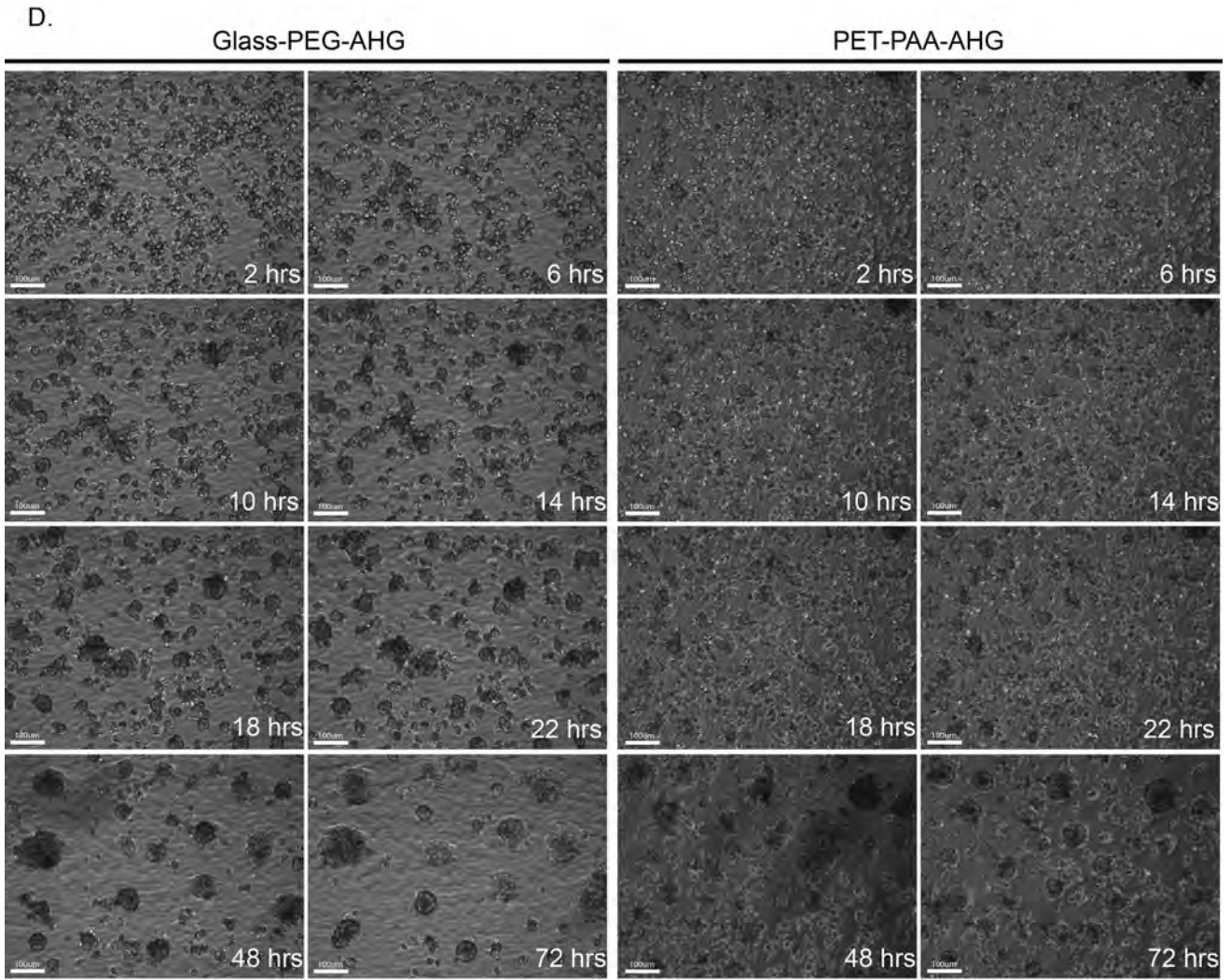


Fig. 2. (continued).

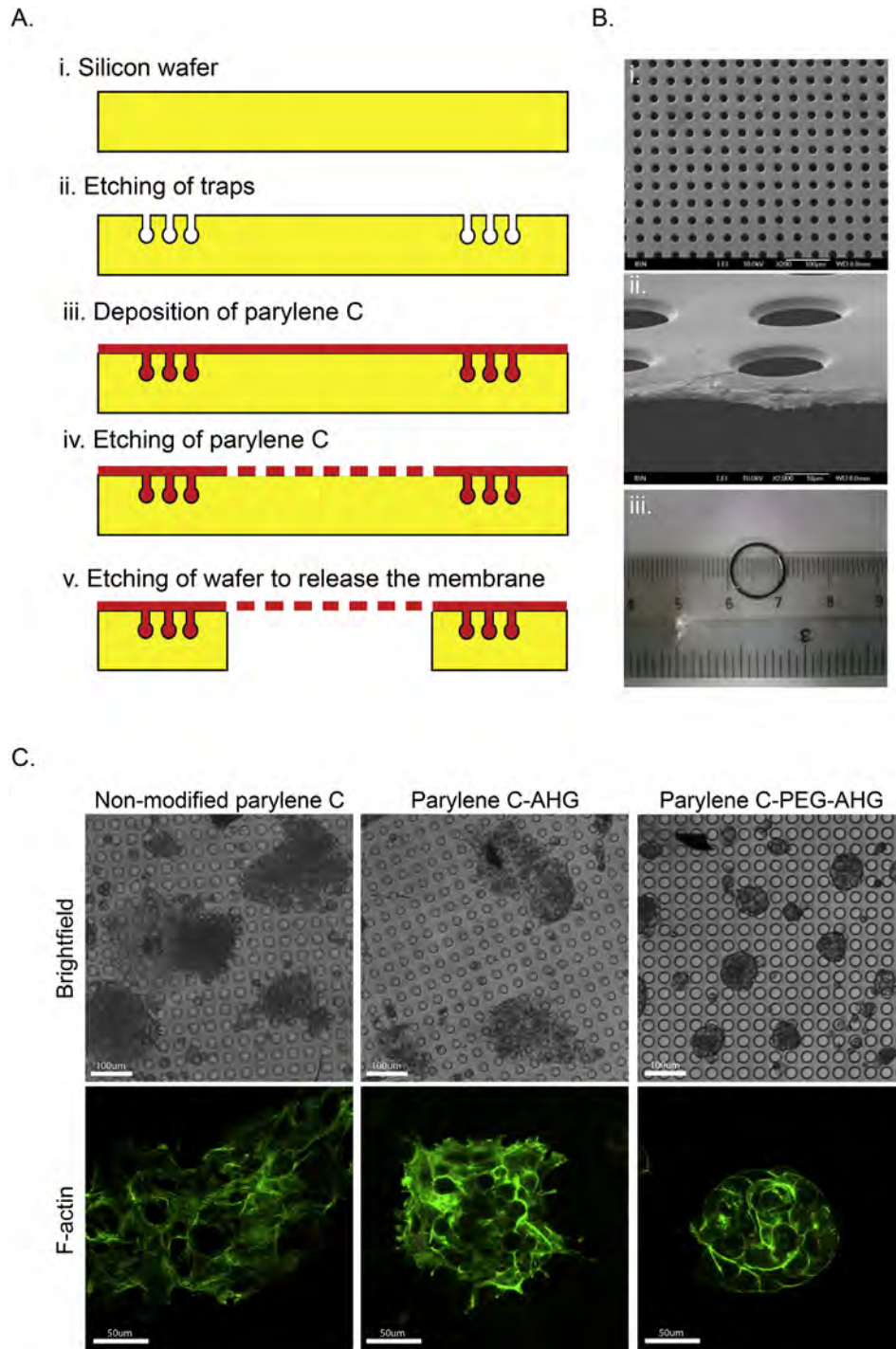


Fig. 3. Fabrication and modification of Parylene C membrane. (A) Fabrication steps for Parylene C membrane. (B) Scanning electron microscope (SEM) and photograph of Parylene C membrane. The Parylene C membrane has uniform pore size and distribution, and is transparent. (C) Brightfield (upper panel) images and F-actin staining (green) on Day 4 indicate that PEG and AHG modification of Parylene C membrane is necessary to preserve spheroid morphology and cytoskeleton distribution. (For interpretation of the references to colour in this figure legend, the reader is referred to the web version of this article.)

2.6. Rat hepatocyte isolation and culture

Primary rat hepatocytes were harvested from male Wistar rats (250–300 g) using a modified two-step *in situ* collagenase perfusion method [33]. Animals were handled according to the Institutional Animal Care and Use Committee (IACUC) protocol approved

by the IACUC of the National University of Singapore. Freshly isolated hepatocytes were seeded onto collagen-coated surfaces or galactose-modified surfaces at 1×10^5 cells/cm². The cells were subsequently cultured in William's E medium supplemented with 1 mg/mL BSA, 10 ng/mL EGF, 0.5 µg/mL insulin, 5 nM dexamethasone, 50 ng/mL linoleic acid, 100 units/mL penicillin and 100 µg/mL

streptomycin; and incubated at 37 °C, under 5% CO₂, and 95% humidity.

2.7. Collagen sandwich culture

To prepare the bottom collagen-coating substrate of the collagen sandwich culture, 40 µL of neutralized collagen type I solution (Vitrogen, Palo Alto, CA) was added onto 10 mm glass coverslips and the coverslips were then incubated at 37 °C overnight. Hepatocytes were then seeded onto the collagen-coated coverslips and allowed to attach for 1 h before additional culture medium was added. Following 24 h of culture, the culture medium was removed and collagen solution was overlaid on top of the cells. Gelation of the collagen overlay was allowed to occur at 37 °C for 3 h before the addition of more culture medium.

2.8. Live imaging of spheroid formation

The dynamics of rat hepatocyte spheroid formation was captured under bright-field microscopy at 10× magnification using the Cell-IQ® MLF system (CM Technologies, Finland). Rat hepatocytes were allowed to attach for 2 h prior to imaging. The built-in incubation chamber was maintained at 37 °C under 5% CO₂.

2.9. Quantification of spheroid formation efficiency

As spheroids form, the substrate surface area covered by cells typically decreases over time. The efficiency of spheroid formation was assessed by measuring the percentage of substrate area covered by cells, using the Cell-IQ® MLF system equipped with the Cell Analyzer Software. Briefly, the software applies proprietary algorithms to identify the areas occupied by cells, and calculates the number of positive (cell-occupied) pixels for every image. The fraction of total surface area covered by cells was then calculated by dividing the number of positive pixels by the total number of pixels per image.

2.10. Scanning electron microscopy (SEM)

The top and cross section of the Parylene C membrane was imaged using SEM (JEOL JSM-5600) at 10 kV. The top section was captured at 200× magnification while the cross section was captured at 2000× magnification. Prior to imaging, the Parylene membrane was dried and sputter-coated with platinum for 60 s.

2.11. Set-up of perfused CS culture system

The perfused CS system set-up is depicted in Fig. 1. Following the harvest and seeding of primary rat hepatocytes, the cells were seeded onto the bottom substrate. The hepatocytes were then cultured for 24 h before being overlaid with the Parylene C membrane. The resulting CS sandwich configuration was secured using a MINUSHEET® tissue carrier (Minucells and Minutissue Vertriebs GmbH, Germany). The entire set-up was then transferred to a laminar flow bioreactor that was developed previously [12]. Perfusion (0.03 mL/min) was implemented in a close-loop format, which consists of the bioreactor, medium reservoir, peristaltic pump (Ismatec SA, Switzerland), stopping valves (Upchurch Scientific, USA) and oxygen-permeable silicone tubing (Ismatec SA, Switzerland). 10 mL of medium was exchanged every 7 days with fresh medium. At the designated time-points, the bioreactors were disassembled and the CS set-up was transferred into multi-well plates for further analysis.

2.12. Immunofluorescence microscopy

At the designated time-points, hepatocytes were fixed with 3.7% paraformaldehyde for 15 min. The cells were then permeabilized with 0.5% Triton X-100 for 30 min and blocked with 1% bovine serum albumin (BSA) in PBS for 1 h. To stain F-actin, cells were incubated in 5 units/mL of AlexaFluor® 488 Phalloidin (Invitrogen, USA) diluted in 1% BSA in PBS for 1 h. To probe for multidrug resistance-associated protein 2 (MRP2), cells were incubated in 50 µg/mL rabbit anti-MRP2 (Sigma Aldrich, USA) diluted in 1% BSA in PBS at 4 °C overnight. The cells were then washed and stained with 40 µg/ml of AlexaFluor® 533 goat anti-rabbit secondary antibody for 3 h protected from light. Confocal microscopy images were acquired using the Olympus Fluoview 300 or Olympus Fluoview 1000 confocal microscope (Olympus, Japan).

2.13. Quantification of spheroid retention

To quantify the degree of spheroid retention, we used DNA content as a surrogate measure of cellularity. Following 8 or 14 days of culture, hepatocytes were lysed with Buffer RLT Plus (Qiagen, Netherlands) and DNA content was quantified using the Quant-iT™ PicoGreen® dsDNA Assay Kit (Invitrogen, USA) according to the manufacturer's protocol. The percentage of hepatocytes retained after culture was calculated by normalizing the DNA content at each time-point to the DNA content on day 2 of culture.

2.14. Quantitative polymerase chain reaction (qPCR)

RNA was isolated using the RNeasy Plus Micro Kit (Qiagen, Netherlands) and converted into cDNA using the High Capacity RNA-to-cDNA Kit (Applied Biosystem, USA) according to the manufacturers' instruction. Primers sequences for *Cyp1a2*, *Cyp2b1/2*, *Cyp3a2*, and *Cyp2c11* are shown in Table 1. RT-PCR was performed using the Fast Start Universal SYBR Green Master (Rox) (Roche, Switzerland) with 10 ng of cDNA sample and the ABI 7500 Fast Real-Time PCR system (Applied Biosystem USA). Gene expression was calculated using the $\Delta\Delta CT$ method normalized to GAPDH.

2.15. Image processing

Quantification of MRP2 localization along the cell boundary (delineated by F-actin) was performed by implementing an image-processing algorithm developed in MATLAB R2011a (Mathworks, Massachusetts). Fluorescence from F-actin staining was first binarized by thresholding segmentation to yield cell boundaries. Distance transform was then performed to compute the Euclidean distance of each pixel in the image to the cell boundaries [49]. Fluorescence from MRP2 staining was also binarized to identify regions where MRP2 was expressed and the total number of positive pixels in the image was measured (I_{total}). For each MRP2-positive pixel, the distance to the closest cell boundary pixel was obtained from the distance transform. Intra-cellular MRP2-positive pixels within a 2-pixel distance from the closest cell boundary pixel

Table 1
Primer sequences used for qPCR measurement.

Gene	Forward sequence	Reverse sequence
<i>GAPDH</i>	AGACAGCCGCATCTTCTGT	TGATGGCAACAATGTCCACT
<i>Cyp1a2</i>	CACGGCTTTCTGACAGACC	CCAAGCCGAAGAGCATCACC
<i>Cyp2b1/2</i>	ACCGGTACCAACCCTTGAT	TGTGTGTTACTCCAATAGGGACAA
<i>Cyp3a2</i>	TGGGACCCGCACACATGGACT	TCCGTGATGGCAAAACAGAGGCA
<i>Cyp2c11</i>	CCCTGGAAGTCATAACCAAG	ACAGTAGCCACCAAGCTTTC
<i>Cyp2d6</i>	TCACACAATGCAATCCGTTT	GCCAGAGATTGAGGCTGCTG

were measured ($I_{\text{localized}}$). The ratio between $I_{\text{localized}}$ and I_{total} was used to quantify the degree of localization of MRP2 along the cell boundary.

For MRP2/CD147 apical-basolateral co-stained samples, XZ and YZ dimensions were visualized using IMARIS. Colocalization, as represented by the Manders' coefficient, were calculated using the Just Another Colocalization Plugin (JACoP) module [50] in ImageJ.

2.16. Quantification of urea and albumin production

The amount of urea produced by the hepatocytes in the culture medium was measured using the Urea Nitrogen Kit (Stanbio Laboratory, USA). The amount of albumin produced was measured using the Rat Albumin ELISA Quantification Kit (Bethyl Laboratories Inc., USA). Levels of urea and albumin production were calculated by normalizing the measured values against the total number of cells.

2.17. Liquid chromatography-mass spectrometry (LC-MS) for metabolites identification

At each designated time-point, CYP-specific substrates (CYP1A2: phenacetine, CYP2B1/2: bupropion, CYP3A2: midazolam) diluted in Krebs-Henseleit buffer (KHB) were added to the cultured hepatocytes for 1.5 h. Hepatocytes in perfusion culture were removed from the bioreactor and transferred to multi-well plates for this experiment. The samples were collected and stored at -80°C until LC-MS could be performed to measure the levels of metabolites produced (CYP1A2: acetaminophen, CYP2B1/2: OH-bupropion, CYP3A2: 1'-OH-midazolam). 50 μL of 100 ng/mL internal standard were added to the samples and the mixtures were dried using the Techne® Sample Concentrator (Techne, UK). The dried residues were then reconstituted using 100 μL of methanol containing 0.1% formic acid. The supernatants were then analysed using LC-MS (LC: 1100 series, Agilent, US; MS: LCQ Deca XP Max, Termo Finnigan, US) with a 100×3.0 mm onyx-monolithic C18 column (Phenomenax, USA) as reported previously [21].

3. Results

3.1. Design and fabrication of the CS culture system

3.1.1. Characterization of bottom glass-PEG-AHG substrate for rapid hepatocyte spheroid formation

It is well-known that primary hepatocytes *in vitro* remain viable only for a few days and rapidly lose their *in vivo* phenotype [51]. In seeking to engineer a transparent low-adhesion substrate that can enable the rapid formation of hepatocyte spheroids, we modified glass coverslips with PEG and AHG (Glass-PEG-AHG). Spheroid formation on Glass-PEG-AHG was compared against the same cells cultured on previously developed PET-PAA-AHG films [21,38,52].

Glass-PEG-AHG was fabricated by sequential conjugation of PEG followed by the AHG galactose moiety (as described in Fig. 2A) onto glass coverslips. The surface modification was verified using XPS analysis (Fig. 2B). Comparing high resolution C1s scans of pristine glass coverslips and PEG-modified glass coverslips, an increase in C–O (shift from 1.5 eV from C–C peaks) was observed, indicating successful conjugation of PEG (Fig. 2Bi and ii). This trend was reversed following the conjugation of AHG as the C–H bond from the moiety was detected (Fig. 2Biii). Additionally, this was confirmed by high resolution N1s scans, which indicated an increase in N element following the conjugation of galactose, as compared to unmodified and PEG-modified glass coverslips (Fig. 2Biv).

To visualize the topography of the modified surfaces, we conducted height measurements using AFM (Fig. 2C). While

Table 2
Roughness and stiffness measurement using AFM.

	Glass	Glass-PEG	PET	PET-pAAc
Roughness (Rq)	0.666 nm	0.636 nm	6.22 nm	3.05 nm
Stiffness (Average)	16.352 GPa	5.245 GPa	2.598 GPa	4.023 GPa

unmodified glass coverslips exhibited a relatively smooth surface, the surface of PEG-modified glass coverslips were smooth with small, evenly distributed elevations. This, in addition to the finding that the average stiffness of glass coverslips dramatically decreased with PEG modification (5.2 GPa) as compared to unmodified glass coverslips (16.4 GPa) (Table 2), indicates that PEG was successfully conjugated to the glass surface. Similar height and stiffness measurements were made on the PET-PAA-AHG substrates [21,38,52]. While the surface roughness of PET and PET-PAA were much higher than Glass and Glass-PEG, the stiffness of Glass-PEG and PET-PAA were of the same magnitude (Table 2).

The dynamics of hepatocyte spheroid formation on the Glass-PEG-AHG substrates were captured using time-lapse imaging and compared to that on the PET-PAA-AHG films (Fig. 2D and Supplementary video). 6 h after seeding, hepatocytes were observed to migrate towards each other to form small aggregates on both Glass-PEG-AHG and PET-PAA-AHG, with greater mobility observed for cells cultured on Glass-PEG-AHG than PET-PAA-AHG. Aggregation of hepatocytes cultured on Glass-PEG-AHG continued over the next 24 h, while hepatocytes cultured on PET-PAA-AHG were more spread-out and formed smaller clusters (with many of them remaining as individual cells). 48 h post-seeding, hepatocytes cultured on Glass-PEG-AHG formed distinct spheroids with clean boundaries but those cultured on PET-PAA-AHG were still aggregate-like. Hepatocytes only formed distinct spheroids on PET-PAA-AHG after 72 h of culture.

Supplementary video related to this article can be found at <http://dx.doi.org/10.1016/j.biomaterials.2015.11.036>.

The degree of spheroid formation was quantified by measuring the area of culture substratum covered by cells (Fig. 2E). In the first 24 h, we observed a steady decrease in the area of Glass-PEG-AHG covered by hepatocytes, while it remained constant for PET-PAA-AHG. The area covered by hepatocytes cultured on PET-PAA-AHG

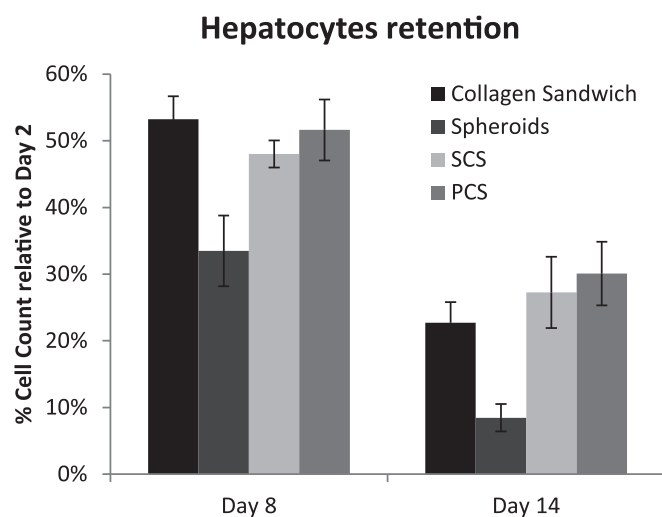


Fig. 4. Retention of hepatocyte spheroids. DNA content was used as a measure of hepatocyte numbers over time in culture. In the presence of the Parylene C membrane overlay, spheroids were better retained. SCS: static CS culture system; PCS: perfused CS culture system.

only started to decrease 30 h post-seeding. It was previously found that PET-PAA-AHG-cultured hepatocytes took up to 72 h to form spheroids [52]. The hepatocytes substratum coverage on PET-PAA-AHG at 72 h is $46 \pm 13\%$, thus 46% was used as a benchmark for

spheroid formation. Our results shows that the substratum coverage for hepatocytes seeded on Glass-PEG-AHG decreased rapidly to $46 \pm 3\%$ within 30 h post-seeding, indicating much more rapid spheroid formation.

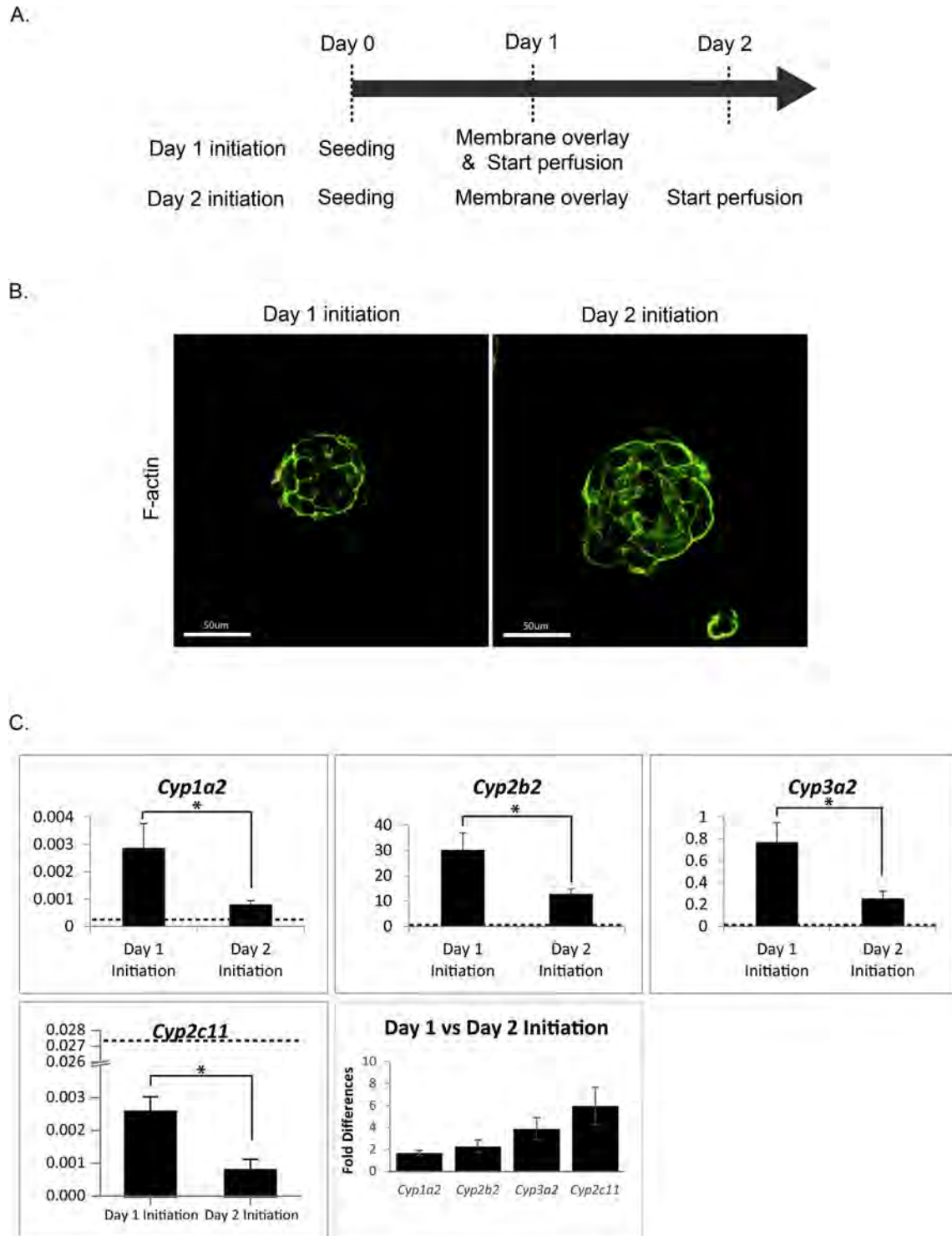


Fig. 5. Earlier initiation of perfusion culture improves CYP gene expression without disrupting cytoskeleton distribution. (A) Experimental set-up to study the effect of perfusion initiation time. (B) F-actin staining of hepatocytes spheroids on Day 7, after 1 or 2 days of static culture prior to the initiation of perfusion. (C) Gene expression of *Cyp1A2*, *Cyp2B2*, *Cyp3A2*, *Cyp2C11* and *Cyp2D6* was much higher on Day 7 when perfusion culture was initiated on Day 1 instead of Day 2. Data plotted represents the mean \pm S.E.M of 3 independent experiments. * $p < 0.05$.

3.1.2. Characterization of top Parylene C membrane overlay

The purpose of the top Parylene C membrane is to mechanically immobilize the pre-formed spheroids on the bottom Glass-PEG-AHG substrate. Given that the Parylene C membrane is thin and flexible, it needs to be held flat by securing its edges. Attaching Parylene C directly to a ring structure using conventional adhesives is not feasible as they are easily removed by ethanol or any other alcohols often used for microfabrication or sterilization process. For this reason, we designed and engineered a device where the Parylene C membrane is mechanically anchored onto a silicon ring (Fig. 3A).

SEM images of the Parylene C membrane indicated that the membrane is perforated with pores of uniform size and distribution (Fig. 3Bi). The thickness of the membrane is approximately 2.5 μm (Fig. 3Bii). Additionally, due to the thinness and low absorption properties in the visible light region, the Parylene C membrane is also transparent, which enables easy imaging (Fig. 3Biii).

Next, given that the mechanical rigidity [53] and/or ligands presented on the surface of substrates [36] can affect the formation of hepatocyte spheroids, we investigated whether additional modification to the Parylene C membrane was necessary. To this end, the Parylene C membrane was modified with either the AHG galactose moiety or PEG-AHG (PEG inclusion to reduce stiffness) and their effects on hepatocyte spheroid formation on Glass-PEG-AHG were examined (Fig. 3C). In the absence of any modification, the placement of unmodified Parylene C above the hepatocyte spheroids resulted in disruption of spheroid structure. Hepatocyte spheroids overlaid with AHG-modified Parylene C remained as aggregates, but cell spreading was observed along the spheroid border. Spheroid structure was best maintained when hepatocyte spheroids were overlaid with the PEG-AHG-modified Parylene C membrane. Besides morphology, the organization of F-actin in the hepatocyte spheroids overlaid by the unmodified and modified Parylene C membranes was also investigated. When overlaid with the unmodified Parylene C membrane, stress fibres in hepatocytes were observed, reminiscent of cells that strongly adhere when cultured on rigid substrates [54]. When overlaid with the AHG-modified Parylene C membrane, filapodia-like structures were observed along the border of hepatocyte spheroids, suggesting that cells along the border were spread out. In contrast, in the presence of the PEG-AHG-modified Parylene C membrane, cortical F-actin was observed in the hepatocyte spheroids, indicating that modification of Parylene C with both PEG and AHG is necessary to preserve hepatocyte spheroidal morphology in the CS culture set-up.

3.2. Retention of spheroids in the CS culture system

To evaluate the effectiveness of the CS configuration in minimizing spheroid loss over time in culture, DNA content was measured at 8 and 14 days after initiation of culture and compared against that at Day 2 (Fig. 4). Results were compared against hepatocytes cultured in the classic collagen sandwich culture system or grown as spheroids on the Glass-PEG-AHG substrate in the absence of the top Parylene C membrane overlay. Strikingly, compared to the unconstrained spheroids, there was significant retention of hepatocyte spheroids cultured in the CS configuration in the presence of the top Parylene C membrane (1.43-fold and 3.22-fold higher after Day 8 and 14, respectively), similar to cells cultured using the collagen sandwich culture system.

3.3. Perfused CS culture system

3.3.1. Optimization of perfusion initiation

Perfusion culture can either be initiated immediately or following a period of static culture. In our previous study, we found

that the inclusion of static culture prior to perfusion initiation is necessary to stabilize the formation of cell–cell contacts, biliary excretion and metabolic functions of collagen sandwich-cultured hepatocytes [12]. Therefore, to optimize the perfusion initiation time in this study, we compared the effect of introducing perfusion after one versus two days of static culture following the establishment of the CS culture system on hepatocyte morphology and function (Fig. 5A).

Interestingly, in contrast to our previous finding, while there were no differences in the distribution of F-actin when hepatocyte spheroids were statically cultured for either one or two days (Fig. 5B), delayed initiation of perfusion in the CS culture system had a detrimental effect on the expression of major drug metabolic enzymes (Fig. 5C). We found that the expression of CYPs on Day 7 was significantly higher when perfusion was initiated earlier. Specifically, when perfusion culture was initiated immediately on Day 1, gene expression was 1.67 ± 0.23 fold higher for *Cyp1A2*, 2.28 ± 0.57 fold higher for *Cyp2B1/2*, 3.88 ± 1.02 fold higher for *Cyp3A2*, and 5.95 ± 1.70 fold higher for *Cyp2C11* as compared to the case where perfusion was initiated on Day 2.

3.3.2. Retention of spheroids under perfusion

Whether for short- or long-term culture, we found that the introduction of perfusion did not increase hepatocyte spheroid loss due to fluid flow. There were no differences in the DNA content

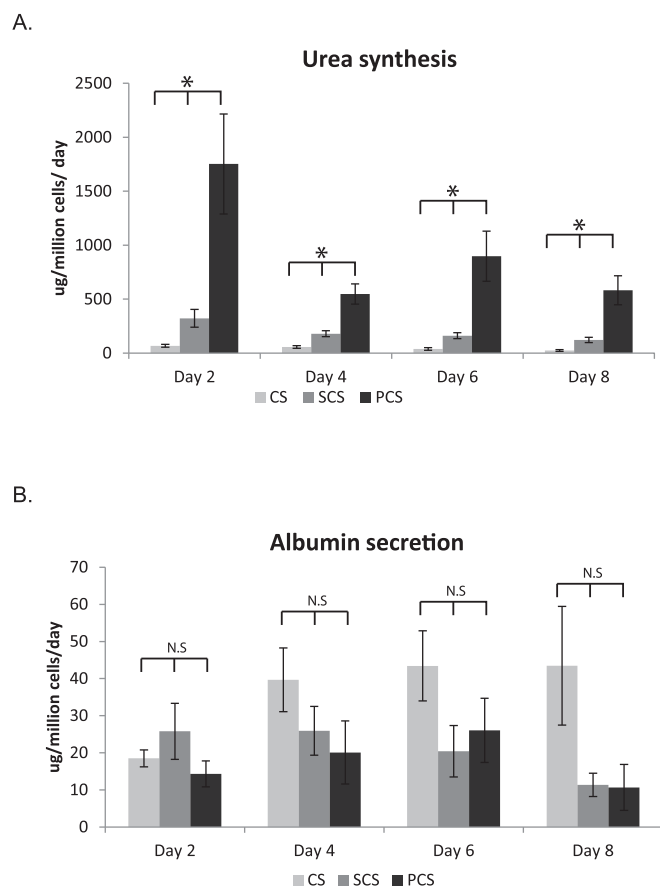
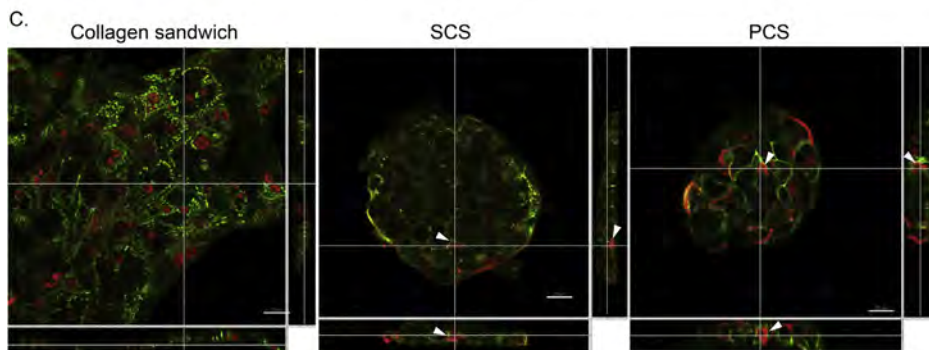
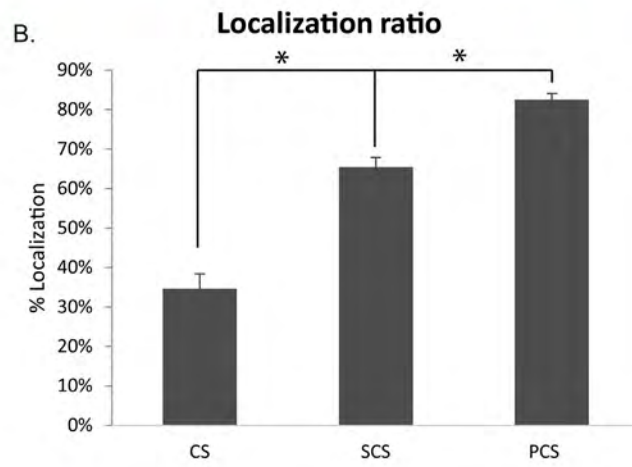
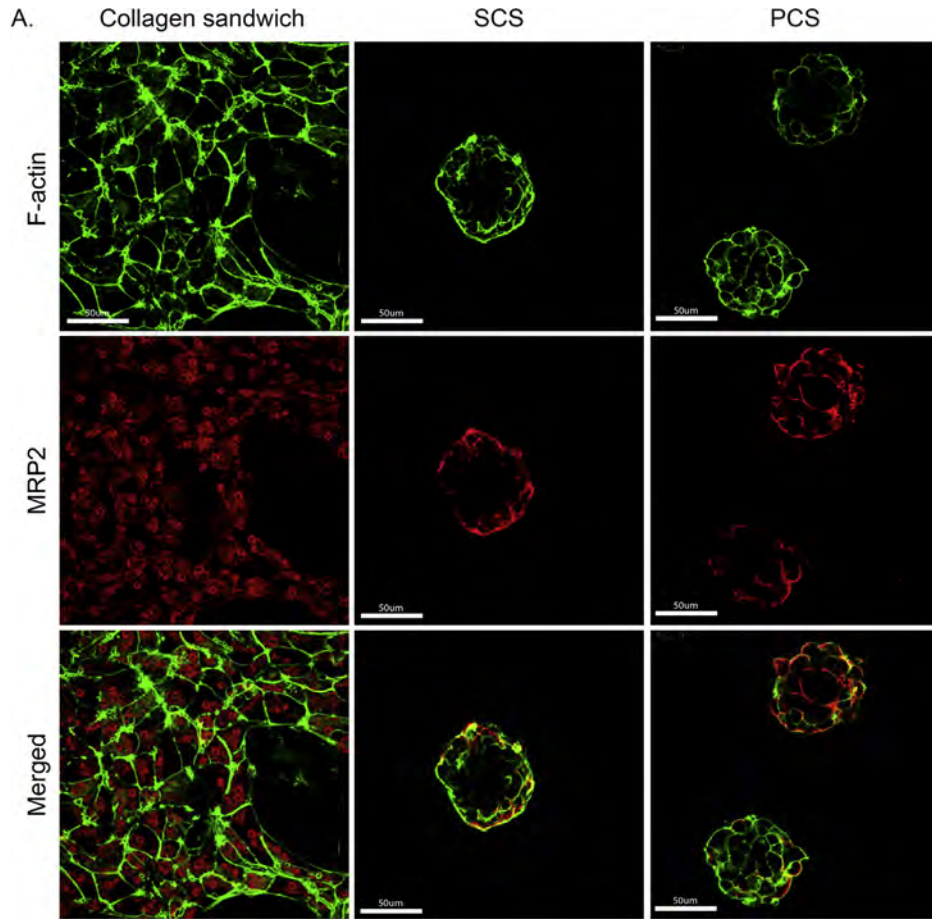


Fig. 6. Urea and albumin production. (A) Urea secretion was significantly higher in SCS and PCS as compared to the collagen sandwich culture. (B) Differences in the amount of albumin secreted were non-significant in SCS and PCS as compared to the collagen sandwich culture. Data plotted represents the mean \pm S.E.M of 3 independent experiments. * $p < 0.05$.



between the static and perfused CS cultures at 8 or 14 days, and DNA content was comparable to that of the collagen sandwich culture (Fig. 4).

3.3.3. Effect of perfusion on urea and albumin synthesis

Within the same CS culture system, the provision of perfusion significantly enhanced urea production in the cultured hepatocyte spheroids (Fig. 6A). While the amount of urea secreted on Day 2, 4, 6 and 8 under static conditions were 322.31 ± 82.39 , 179.97 ± 28.19 , 161.6 ± 27.69 and 121.62 ± 24.56 $\mu\text{g}/\text{million cells}/\text{day}$, urea production under perfusion was three- to five-fold higher at 1752.38 ± 462.48 , 547.87 ± 93.47 , 898.06 ± 231.22 and 582.68 ± 134.09 $\mu\text{g}/\text{million cells}/\text{day}$ over the same time-points. Notably, whether in the static or perfused CS culture system, urea production was significantly greater as compared to hepatocytes cultured in the classic collagen sandwich culture system at all time-points (Fig. 6A).

In contrast, the provision of perfusion did not have an effect on albumin secretion (Fig. 6B). Furthermore, whether in the static (range: 11.36 ± 3.148 to 25.79 ± 7.55 $\mu\text{g}/\text{million cells}/\text{day}$) or perfused (range: 10.67 ± 6.19 to 26.03 ± 8.64 $\mu\text{g}/\text{million cells}/\text{day}$) CS culture system, albumin production was comparable to that of cells cultured in the collagen sandwich culture system (range: 18.51 ± 2.27 to 43.45 ± 16.01 $\mu\text{g}/\text{million cells}/\text{day}$) (Fig. 6B).

3.3.4. Effect of perfusion on maintenance of polarity

In polarized hepatocytes, MRP2 localizes specifically to the apical membrane [55]. With the loss of polarity, internalization of MRP2 is observed [56,57] [58]. Using the cellular localization of MRP2 as an indicator of hepatocyte polarity, we probed for F-actin and MRP2 in the hepatocytes to identify the cell boundary and location of MRP2 respectively. Through immunostaining, we observed that the degree of MRP2 localization to the cell boundary was higher under perfusion as compared to static culture (Fig. 7A). Furthermore, whether in the static or perfused CS culture system, MRP2 was more localized to the cell boundary as compared to the same cells grown in the collagen sandwich culture system. Indeed, these findings were confirmed using an image analysis algorithm, where quantification of MRP2 localization indicated that the percentage of MRP2 detected at the cell boundary was significantly higher in the perfused CS culture ($82.54 \pm 1.58\%$) as compared to the static CS sandwich culture ($65.45 \pm 2.44\%$) and the collagen sandwich culture ($34.68 \pm 3.69\%$) (Fig. 7B).

To further verify the apical localization of MRP2, we probed for CD147 (a basolateral marker) in addition to MRP2. MRP2 was found to be located in spatially distinct domains from CD147 in hepatocytes cultured under static or perfused conditions in the CS culture system, indicating formation of distinct apical-basolateral polarity (Fig. 7C). In contrast, MRP2 was detected mainly in the nucleus in collagen sandwich-cultured hepatocytes, suggesting the loss of hepatocyte polarity. Further, we quantified the degree of MRP2/CD147 colocalization using the JACoP module in ImageJ, where the Manders' coefficients of '0' and '1' correspond to no overlap and 100% co-localization, respectively. The Manders' coefficient for the collagen sandwich culture, static and perfused CS sandwich culture were found to be 0.598, 0.299 and 0.262 respectively, confirming that apical-basolateral polarity was best maintained in the perfused

CS sandwich culture system.

3.3.5. Effect of perfusion on CYP metabolic activity

The metabolic activity of CYP1A2, CYP2B1/2 and CYP3A2 was measured by quantifying the amount of metabolites produced in the presence of enzyme-specific substrates. While the provision of perfusion in the CS culture system did not increase CYP1A2 activity over static culture at Day 8 as evidenced by the amount of acetaminophen produced (perfusion: 99.97 ± 8.57 $\text{ng}/\text{million cells}/90$ min, static: 127.09 ± 18.16 $\text{ng}/\text{million cells}/90$ min), CYP1A2 activities in both static and perfused CS cultures were still significantly greater than that in the collagen sandwich cultured-hepatocytes (52.43 ± 7.48 $\text{ng}/\text{million cells}/90$ min). Similar findings were observed at Day 14, where the amount of acetaminophen measured in the static and perfused CS cultures were 88.12 ± 8.27 and 95.73 ± 10.36 $\text{ng}/\text{million cells}/90$ min, respectively. In comparison, only 26.98 ± 2.60 $\text{ng}/\text{million cells}/90$ min of acetaminophen was measured in the collagen sandwich-cultured hepatocytes (Fig. 8A).

The provision of perfusion in the CS culture system significantly enhanced the metabolic activity of CYP2B1/2 as compared to static culture at Day 8 as evidenced by the amount of OH-bupropion metabolized from bupropion (perfusion: 17.76 ± 1.34 $\text{ng}/\text{million cells}/90$ min, static: 7.45 ± 0.42 $\text{ng}/\text{million cells}/90$ min). The amount of OH-bupropion produced by the collagen sandwich cultured-hepatocytes (8.97 ± 0.67 $\text{ng}/\text{million cells}/90$ min) was similar to the levels measured in the static CS culture system. Similarly, on Day 14, we observed a trend of increased OH-bupropion production in the perfused CS sandwich culture system as compared to static culture but this difference was not statistically significant (Fig. 8B).

Lastly, the provision of perfusion in the CS culture system also significantly enhanced the metabolic activity of CYP3A2 as compared to static culture at Day 8 as evidenced by the amount of 1'-OH-midazolam metabolized by CYP3A2 from midazolam (perfusion: 28.74 ± 5.98 $\text{ng}/\text{million cells}/90$ min, static: 8.28 ± 1.59 $\text{ng}/\text{million cells}/90$ min). The amount of 1'-OH-midazolam produced by the collagen sandwich cultured-hepatocytes (10.78 ± 1.43 $\text{ng}/\text{million cells}/90$ min) was similar to the levels measured in the static CS culture system. Similar findings were observed at Day 14, where the amount of 1'-OH-midazolam measured in the perfused CS cultures was 37.57 ± 11.8 $\text{ng}/\text{million cells}/90$ min. In comparison, only 12.31 ± 3.92 and 7.79 ± 2.39 $\text{ng}/\text{million cell}/90$ min of 1'-OH-midazolam was measured in the static CS culture and collagen sandwich culture, respectively (Fig. 8C).

4. Discussion

Despite the numerous advantages associated with growing hepatocytes *in vitro* as spheroids, this approach has yet been optimized for high throughput drug screening due to variations mainly attributed to the loss of spheroids during culture. Ideally, a hepatocyte spheroid culture system amenable to drug testing should minimize spheroid loss during culture, provide size control of cultured spheroids, and promote adequate mass transfer (via perfusion) that facilitates nutrient and waste exchange. In seeking to address the following key requirements, we asked if the

Fig. 7. Maintenance of hepatocyte polarity (A) F-actin (green) and MRP2 (red) stained hepatocyte spheroids cultured in SCS, PCS or collagen sandwich culture system. MRP2 localization along the cell border (delineated by F-actin staining) was markedly improved in SCS and PCS on Day 8 as compared to the collagen sandwich culture system. (B) Degree of MRP2 and F-actin staining co-localization. Image quantification shows that MRP2 localization was 2.4 times higher in PCS and 1.9 times higher in SCS as compared to the collagen sandwich culture. Data plotted represents the mean \pm S.E.M. * $p < 0.05$. (C) MRP2 (red) and CD147 (green) expression in SCS, PCS or collagen sandwich culture system. Staining for MRP2 and CD147 was in spatially distinct regions in hepatocyte in SCS and PCS on Day 8 as indicated by the white arrows. (For interpretation of the references to colour in this figure legend, the reader is referred to the web version of this article.)

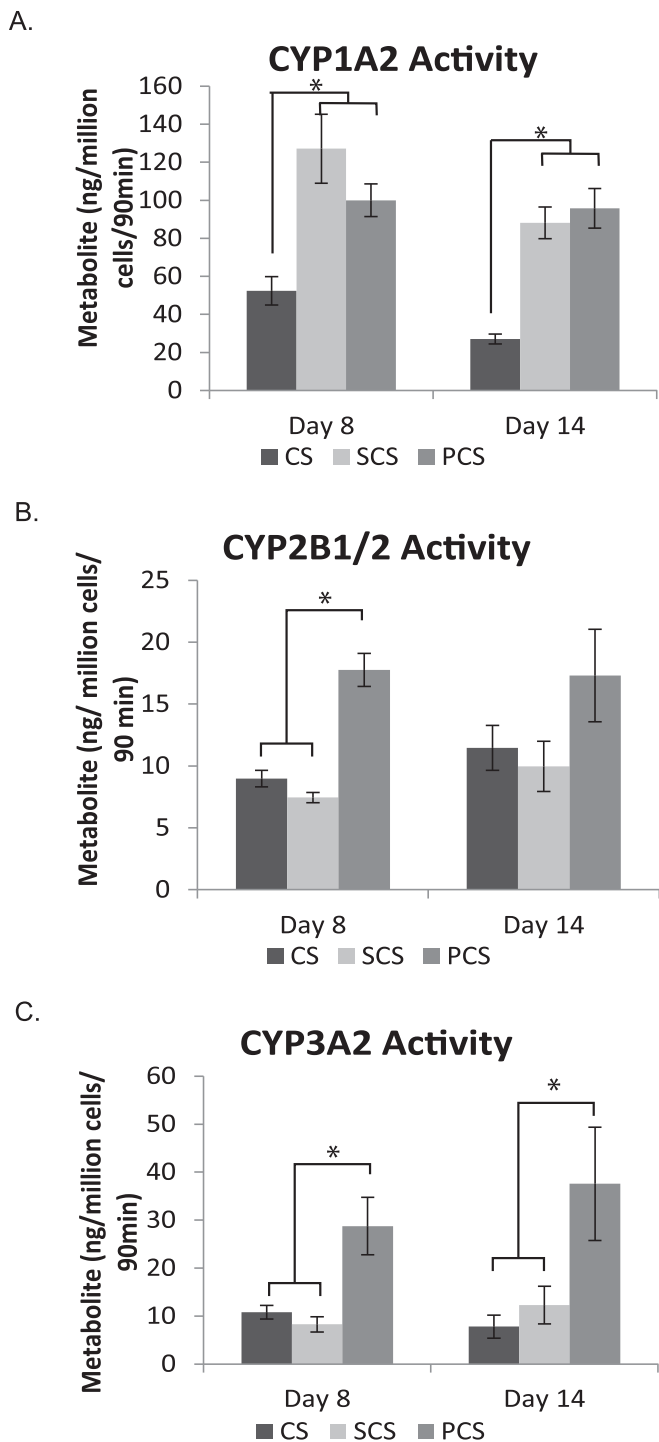


Fig. 8. CYP metabolic activities. (A) CYP1A2 activity, measured by the amount of acetaminophen metabolized from phenacetine. (B) CYP2B1/2 activity, measured by the amount of OH-bupropion metabolized from bupropion. (C) CYP3A2 activity, measured by the amount of 1'-OH-medazolam metabolized from midazolam.

implementation of physical restraint in the form of a sandwich configuration would minimize cell loss and enable perfusion culture. We report that the overlay of an ultrathin microfabricated porous membrane on hepatocyte spheroids cultured on a low-adhesion Glass-PEG-AHG coverslip is an effective means of mechanically immobilizing the spheroids and hence minimizing spheroid loss during culture. Additionally, as this physical

constraint prevents spheroids from coalescing into larger spheroids over time, tight control over spheroid size is also achieved. Lastly, as the CS culture system is also amenable to perfusion culture, we sought to evaluate the effect of perfusion and found that perfusion not only enhanced urea secretion and CYP metabolic activity, but also better maintained hepatocyte polarity as compared to cells in static culture and the collagen sandwich culture.

Parylene C was selected as the material to fabricate the top membrane overlay as it possesses multiple favourable features. First, it is a Food and Drug Administration (FDA) Class IV-approved material widely used to coat medical implants [59,60]. Additionally, it exhibits good chemical stability which minimizes potential interference to downstream drug testing. As crystalline Parylene C is optically transparent to visible light [61], direct microscopic observation under bright-field and image-based drug screening experiments can be conducted. In contrast to conventional polymeric materials, Parylene C can be deposited using chemical vapour deposition (CVD) which enables the formation of pinhole-free thin layers with controllable thickness. Indeed, the Parylene C membrane fabricated in this study was only 2 μm in thickness; therefore, the membrane facilitates adequate mass transfer while protecting the hepatocytes from flow-induced shear stress during perfusion. Furthermore, Parylene C can be fabricated using MEMS [62–64] and is modifiable with oxygen plasma for ligand conjugation [65]. In this study, we demonstrate the necessity for Parylene C-modification with PEG and AHG galactose moiety, consistent with previous findings that mechanical rigidity and ligand presentation [53,66] are key parameters that can influence the formation of hepatocyte spheroids.

Following the optimization of both top (Parylene-PEG-AHG) and bottom (Glass-PEG-AHG) substrates that enable the rapid formation and maintenance of hepatocyte spheroids, the ability of the CS configuration to minimize spheroid loss during static and perfusion culture enabled us to study the effect of perfusion on hepatocyte function, polarity and CYP metabolic activity. Delaying perfusion initiation to hepatocytes cultured in a modified collagen sandwich culture was previously shown to be beneficial to the maintenance of hepatocyte polarity and albumin production [12]. In contrast, in this study, we found that the mRNA levels of several CYPs in the hepatocyte spheroids were significantly reduced with delayed perfusion initiation. This observed difference indicates that the need for pre-stabilization in static culture prior to perfusion is dependent on the culture configuration. While a period of static culture was necessary for the establishment of repolarization cues in the modified collagen sandwich culture [12], our study suggests that this may not be necessary when hepatocytes are grown as spheroids. Rather, the minimization of mass transport problems via a shorter perfusion initiation time may be more critical with spheroid culture.

Following the optimization of conditions for perfusion, we found that urea secretion was improved in the presence of perfusion while no differences in albumin synthesis was detected. In a previous study, Powers and colleagues [67] reported that the rates of urea and albumin production of primary rat hepatocyte aggregates were much greater under perfusion in a microarray bioreactor as compared to static culture. While the results for urea production in our study is consistent with that of Powers and colleagues, the absence of improved albumin secretion warrants further investigation.

Hepatocyte polarity strongly influences xenobiotic uptake and excretion [68]. Typically, primary hepatocytes rapidly lose polarity upon isolation and adequate culture conditions are necessary for the reestablishment of hepatocyte polarity. For example, the current *in vitro* gold standard, the collagen sandwich culture system, has been shown to be capable of reestablishing and maintaining

polarity in primary rat hepatocytes for up to 5 days [58,69]. Furthermore, it has also been reported that spheroid culture better maintains hepatocyte polarity as compared to sandwich culture [70]. Using the apical membrane localization of MRP2 as an indicator of polarity reestablishment, hepatocyte polarity was found to be best maintained in the perfused CS culture system as compared to static culture or in the collagen sandwich culture system. Interestingly, we found that perfusion did not have an effect on hepatocyte repolarization in our previous study, where hepatocytes were cultured in a modified collagen sandwich culture in a perfusion bioreactor [12]. Though these are inherently different systems, that perfusion appears to have an effect on repolarization only when hepatocytes are grown as spheroids necessitates more detailed examination in future studies.

To demonstrate the applicability of the CS culture system for drug metabolism studies, the activity of CYP1A2, CYP2B1/2 and CYP3A2 enzymes were tested under static and perfusion conditions, and compared to the collagen sandwich culture. These CYPs are rat homologs of human CYP1A2, CYP2B6, and CYP3A4 [71,72] respectively and were selected for investigation in this study due to their important roles in drug metabolism. CYP1A2 is the second most abundant CYP in humans and is inducible by many carcinogens and aromatic hydrocarbons [73]; CYP2B6, although accounting for only 5% of total CYPs, is responsible for the metabolism of more than 25% of commercially available drugs [13]; CYP3A4 is the most abundant CYP in humans and is responsible for the metabolism of two-thirds of commercially available drugs [48]. While hepatocyte spheroids cultured in the static CS culture system exhibited higher CYP1A2 activity (but not CYP2B1/2 and CYP3A2 activity) as compared to those cultured in the collagen sandwich culture system, cells under perfusion displayed higher metabolic activity for all three CYPs. In a recent study by Dash and colleagues [74], rat hepatocytes cultured under perfusion in a modified collagen sandwich culture exhibited higher levels of basal CYP activity as compared to the same cells in static culture. Our findings corroborate that of Dash et al. in that perfusion is necessary to maintain hepatocyte metabolism *in vitro*. Since the present study clearly demonstrates the positive effect of perfusion culture, ongoing investigations are examining the mass transport properties in the spheroids under static and perfusion conditions within our CS culture system.

5. Conclusion

We have developed a CS culture system that minimizes the loss of hepatocyte spheroids during culture through the use of a porous ultra-thin membrane to mechanically immobilize the spheroids. Both the bottom (glass coverslip) and top (Parylene C membrane) substrates were specifically modified with PEG and AHG galactose moiety to maintain the architecture of spheroids. Cultured hepatocyte spheroids under static conditions exhibited improved polarity and liver-specific functions that were further enhanced with perfusion as compared to those grown in the standard collagen sandwich culture system. This CS culture system therefore provides a promising platform for the rapid evaluation of drug bioavailability and hepatotoxicity.

Acknowledgement

We thank core facilities in A*STAR, NUHS and MBI for technical support. This work is supported in part by Institute of Bioengineering and Nanotechnology, & grants from JCO-DP, A*STAR; MBI, NMRC, SMART, NUHS and Janssen to H.Y.

W.H.T. and B.N. were NGS scholars, and J.Y. a SMART scholar.

References

- [1] F.P. Guengerich, Cytochrome P450s and other enzymes in drug metabolism and toxicity, *AAPS J.* 8 (2006) E101–E111.
- [2] R. Glockner, P. Steinmetzer, C. Drobner, D. Muller, Application of cryopreserved precision-cut liver slices in pharmacotoxicology—principles, literature data and own investigations with special reference to CYP1A1-mRNA induction, *Exp. Toxicol. Pathol.* 50 (1998) 440–449.
- [3] S.C. Khojasteh, S. Prabhu, J.R. Kenny, J.S. Halladay, A.Y. Lu, Chemical inhibitors of cytochrome P450 isoforms in human liver microsomes: a re-evaluation of P450 isoform selectivity, *Eur. J. Drug Metab. Pharmacokinet.* 36 (2011) 1–16.
- [4] M.T. Donato, A. Lahoz, J.V. Castell, M.J. Gomez-Lechon, Cell lines: a tool for *in vitro* drug metabolism studies, *Curr. Drug Metab.* 9 (2008) 1–11.
- [5] T.B. Andersson, K.P. Kanebratt, J.G. Kenna, The HepaRG cell line: a unique *in vitro* tool for understanding drug metabolism and toxicology in human, *Expert Opin. Drug Metab. Toxicol.* 8 (2012) 909–920.
- [6] N.J. Hewitt, M.J. Lechon, J.B. Houston, D. Hallifax, H.S. Brown, P. Maurel, et al., Primary hepatocytes: current understanding of the regulation of metabolic enzymes and transporter proteins, and pharmaceutical practice for the use of hepatocytes in metabolism, enzyme induction, transporter, clearance, and hepatotoxicity studies, *Drug Metab. Rev.* 39 (2007) 159–234.
- [7] E.L. LeCluyse, P.L. Bullock, A. Parkinson, Strategies for restoration and maintenance of normal hepatic structure and function in long-term cultures of rat hepatocytes, *Adv. Drug Deliv. Rev.* 22 (1996) 133–186.
- [8] J.C. Wanson, P. Drochmans, R. Mosselmans, M.F. Ronveaux, Adult rat hepatocytes in primary monolayer culture. Ultrastructural characteristics of intercellular contacts and cell membrane differentiations, *J. Cell Biol.* 74 (1977) 858–877.
- [9] J.C. Dunn, R.G. Tompkins, M.L. Yarmush, Long-term *in vitro* function of adult hepatocytes in a collagen sandwich configuration, *Biotechnol. Prog.* 7 (1991) 237–245.
- [10] J.C. Dunn, M.L. Yarmush, H.G. Koebe, R.G. Tompkins, Hepatocyte function and extracellular matrix geometry: long-term culture in a sandwich configuration, *FASEB J.* 3 (1989) 174–177.
- [11] B.S. Kim, D.J. Mooney, Development of biocompatible synthetic extracellular matrices for tissue engineering, *Trends Biotechnol.* 16 (1998) 224–230.
- [12] L. Xia, S. Ng, R. Han, X. Tuo, G. Xiao, H.L. Leo, et al., Laminar-flow immediate-overlay hepatocyte sandwich perfusion system for drug hepatotoxicity testing, *Biomaterials* 30 (2009) 5927–5936.
- [13] N.J. Hewitt, R. de Kanter, E. LeCluyse, Induction of drug metabolizing enzymes: a survey of *in vitro* methodologies and interpretations used in the pharmaceutical industry—do they comply with FDA recommendations? *Chem. Biol. Interact.* 168 (2007) 51–65.
- [14] S.F. Abu-Absi, J.R. Friend, L.K. Hansen, W.S. Hu, Structural polarity and functional bile canaliculi in rat hepatocyte spheroids, *Exp. Cell Res.* 274 (2002) 56–67.
- [15] N. Koide, K. Sakaguchi, Y. Koide, K. Asano, M. Kawaguchi, H. Matsushima, et al., Formation of multicellular spheroids composed of adult rat hepatocytes in dishes with positively charged surfaces and under other nonadherent environments, *Exp. Cell Res.* 186 (1990) 227–235.
- [16] F.J. Wu, J.R. Friend, C.C. Hsiao, M.J. Zilliox, W.J. Ko, F.B. Cerra, et al., Efficient assembly of rat hepatocyte spheroids for tissue engineering applications, *Biotechnol. Bioeng.* 50 (1996) 404–415.
- [17] F.J. Wu, J.R. Friend, R.P. Rimmel, F.B. Cerra, W.S. Hu, Enhanced cytochrome P450 IA1 activity of self-assembled rat hepatocyte spheroids, *Cell Transpl.* 8 (1999) 233–246.
- [18] Y. Sakai, S. Yamagami, K. Nakazawa, Comparative analysis of gene expression in rat liver tissue and monolayer- and spheroid-cultured hepatocytes, *Cells Tissues Organs* 191 (2010) 281–288.
- [19] C.M. Brophy, J.L. Luebke-Wheeler, B.P. Amiot, H. Khan, R.P. Rimmel, P. Rinaldo, et al., Rat hepatocyte spheroids formed by rocked technique maintain differentiated hepatocyte gene expression and function, *Hepatology* 49 (2009) 578–586.
- [20] R. Takahashi, H. Sonoda, Y. Tabata, A. Hisada, Formation of hepatocyte spheroids with structural polarity and functional bile canaliculi using nanopillar sheets, *Tissue Eng. Part A* 16 (2010) 1983–1995.
- [21] L. Xia, R.B. Sakban, Y. Qu, X. Hong, W. Zhang, B. Nugraha, et al., Tethered spheroids as an *in vitro* hepatocyte model for drug safety screening, *Biomaterials* 33 (2012) 2165–2176.
- [22] B. Nugraha, X. Hong, X. Mo, L. Tan, W. Zhang, P.M. Chan, et al., Galactosylated cellulosic sponge for multi-well drug safety testing, *Biomaterials* 32 (2011) 6982–6994.
- [23] E.L. LeCluyse, R.P. Witek, M.E. Andersen, M.J. Powers, Organotypic liver culture models: meeting current challenges in toxicity testing, *Crit. Rev. Toxicol.* 42 (2012) 501–548.
- [24] P. Gunness, D. Mueller, V. Shevchenko, E. Heinzle, M. Ingelman-Sundberg, F. Noor, 3D organotypic cultures of human HepaRG cells: a tool for *in vitro* toxicity studies, *Toxicol. Sci.* 133 (2013) 67–78.
- [25] F. Sarvi, T. Arbatan, P.P.Y. Chan, W. Shen, A novel technique for the formation of embryoid bodies inside liquid marbles, *RSC Adv.* 3 (2013) 14501–14508.
- [26] K. Nakazawa, Y. Izumi, J. Fukuda, T. Yasuda, Hepatocyte spheroid culture on a polydimethylsiloxane chip having microcavities, *J. Biomater. Sci. Polym. Ed.* 17 (2006) 859–873.

- [27] H. Hardelauf, J.-P. Frimat, J.D. Stewart, W. Schormann, Y.-Y. Chiang, P. Lampen, et al., Microarrays for the scalable production of metabolically relevant tumour spheroids: a tool for modulating chemosensitivity traits, *Lab Chip* 11 (2011) 419–428.
- [28] M.-J. Yang, C.-H. Chen, P.-J. Lin, C.-H. Huang, W. Chen, H.-W. Sung, Novel method of forming human embryoid bodies in a polystyrene dish surface-coated with a temperature-responsive methylcellulose hydrogel, *Biomacromolecules* 8 (2007) 2746–2752.
- [29] L. Ying, C. Yin, R.X. Zhuo, K.W. Leong, H.Q. Mao, E.T. Kang, et al., Immobilization of galactose ligands on acrylic acid graft-copolymerized poly(ethylene terephthalate) film and its application to hepatocyte culture, *Biomacromolecules* 4 (2003) 157–165.
- [30] T.M. Walker, P.C. Rhodes, C. Westmoreland, The differential cytotoxicity of methotrexate in rat hepatocyte monolayer and spheroid cultures, *Toxicol In Vitro* 14 (2000) 475–485.
- [31] R. Glicklis, J.C. Merchuk, S. Cohen, Modeling mass transfer in hepatocyte spheroids via cell viability, spheroid size, and hepatocellular functions, *Biotechnol. Bioeng.* 86 (2004) 672–680.
- [32] Y. Yamashita, M. Shimada, E. Tsujita, S. Tanaka, H. Iijima, K. Nakazawa, et al., Polyurethane foam/spheroid culture system using human hepatoblastoma cell line (Hep G2) as a possible new hybrid artificial liver, *Cell Transpl.* 10 (2001) 717–722.
- [33] H. Iijima, K. Nakazawa, S. Koyama, M. Kaneko, T. Matsushita, T. Gion, et al., Development of a hybrid artificial liver using a polyurethane foam/hepatocyte-spheroid packed-bed module, *Int. J. Artif. Organs* 23 (2000) 389–397.
- [34] J. Lee, M.J. Cuddihy, G.M. Cater, N.A. Kotov, Engineering liver tissue spheroids with inverted colloidal crystal scaffolds, *Biomaterials* 30 (2009) 4687–4694.
- [35] J.P. Chen, C.T. Lin, Dynamic seeding and perfusion culture of hepatocytes with galactosylated vegetable sponge in packed-bed bioreactor, *J. Biosci. Bioeng.* 102 (2006) 41–45.
- [36] C.S. Cho, S.J. Seo, I.K. Park, S.H. Kim, T.H. Kim, T. Hoshiba, et al., Galactose-carrying polymers as extracellular matrices for liver tissue engineering, *Biomaterials* 27 (2006) 576–585.
- [37] H.F. Lu, W.S. Lim, J. Wang, Z.Q. Tang, P.C. Zhang, K.W. Leong, et al., Galactosylated PVDF membrane promotes hepatocyte attachment and functional maintenance, *Biomaterials* 24 (2003) 4893–4903.
- [38] C. Yin, L. Ying, P.C. Zhang, R.X. Zhuo, E.T. Kang, K.W. Leong, et al., High density of immobilized galactose ligand enhances hepatocyte attachment and function, *J. Biomed. Mater. Res.* A 67 (2003) 1093–1104.
- [39] Y. Du, S.M. Chia, R. Han, S. Chang, H. Tang, H. Yu, 3D hepatocyte monolayer on hybrid RGD/galactose substratum, *Biomaterials* 27 (2006) 5669–5680.
- [40] Y. Du, R. Han, F. Wen, S. Ng San San, L. Xia, T. Wohland, et al., Synthetic sandwich culture of 3D hepatocyte monolayer, *Biomaterials* 29 (2008) 290–301.
- [41] K.N. Chua, W.S. Lim, P. Zhang, H. Lu, J. Wen, S. Ramakrishna, et al., Stable immobilization of rat hepatocyte spheroids on galactosylated nanofiber scaffold, *Biomaterials* 26 (2005) 2537–2547.
- [42] R.G. Wells, The role of matrix stiffness in regulating cell behavior, *Hepatology* 47 (2008) 1394–1400.
- [43] J.L. Walgren, M.D. Mitchell, D.C. Thompson, Role of metabolism in drug-induced idiosyncratic hepatotoxicity, *Crit. Rev. Toxicol.* 35 (2005) 325–361.
- [44] A.W. Tilles, H. Baskaran, P. Roy, M.L. Yarmush, M. Toner, Effects of oxygenation and flow on the viability and function of rat hepatocytes cocultured in a microchannel flat-plate bioreactor, *Biotechnol. Bioeng.* 73 (2001) 379–389.
- [45] G. Mattei, S. Giusti, A. Ahluwalia, Design criteria for generating physiologically relevant in vitro models in bioreactors, *Processes* 2 (2014) 548–569.
- [46] R.M. Tostoes, S.B. Leite, J.P. Miranda, M. Sousa, D.I. Wang, M.J. Carrondo, et al., Perfusion of 3D encapsulated hepatocytes – a synergistic effect enhancing long-term functionality in bioreactors, *Biotechnol. Bioeng.* 108 (2011) 41–49.
- [47] M.A. Findeis, Stepwise synthesis of a galnac-containing cluster glycoside ligand of the asialoglycoprotein receptor, *Int. J. Pept. Protein Res.* 43 (1994) 477–485.
- [48] K.A. Shaw, Z.L. Zhang, N.C. MacDonald, SCREAM I: A single mask, single-crystal silicon, reactive ion etching process for microelectromechanical structures, *Sens. Actuators A Phys.* 40 (1994) 63–70.
- [49] C.R. Maurer Jr., R. Qi, V. Raghavan, A linear time algorithm for computing exact Euclidean distance transforms of binary images in arbitrary dimensions, *IEEE Trans. Pattern Anal. Mach. Intell.* 25 (2003) 265–270.
- [50] S. Bolte, F.P. Cordelieres, A guided tour into subcellular colocalization analysis in light microscopy, *J. Microsc.* 224 (2006) 213–232.
- [51] M.J. Gómez-Lechón, R. Jover, T. Donato, X. Ponsoda, C. Rodríguez, K.G. Stenzel, et al., Long-term expression of differentiated functions in hepatocytes cultured in three-dimensional collagen matrix, *J. Cell. Physiol.* 177 (1998) 553–562.
- [52] Y. Du, R. Han, S. Ng, J. Ni, W. Sun, T. Wohland, et al., Identification and characterization of a novel prespheroid 3-dimensional hepatocyte monolayer on galactosylated substratum, *Tissue Eng.* 13 (2007) 1455–1468.
- [53] A.A. Chen, S.R. Khetani, S. Lee, S.N. Bhatia, K.J. Van Vliet, Modulation of hepatocyte phenotype in vitro via chemomechanical tuning of polyelectrolyte multilayers, *Biomaterials* 30 (2009) 1113–1120.
- [54] P.C. Georges, P.A. Janmey, Cell type-specific response to growth on soft materials, *J. Appl. Physiol.* 98 (2005) 1547–1553.
- [55] J. König, A.T. Nies, Y. Cui, I. Leier, D. Keppler, Conjugate export pumps of the multidrug resistance protein (MRP) family: localization, substrate specificity, and MRP2-mediated drug resistance, *Biochim. Biophys. Acta* 1461 (1999) 377–394.
- [56] H. Kojima, A.T. Nies, J. König, W. Hagmann, H. Spring, M. Uemura, et al., Changes in the expression and localization of hepatocellular transporters and radixin in primary biliary cirrhosis, *J. Hepatol.* 39 (2003) 693–702.
- [57] A.D. Mottino, J. Cao, L.M. Veggi, F. Crocenzi, M.G. Roma, M. Vore, Altered localization and activity of canalicular Mrp2 in estradiol-17beta-D-glucuronide-induced cholestasis, *Hepatology* 35 (2002) 1409–1419.
- [58] P. Zhang, X. Tian, P. Chandra, K.L. Brouwer, Role of glycosylation in trafficking of Mrp2 in sandwich-cultured rat hepatocytes, *Mol. Pharmacol.* 67 (2005) 1334–1341.
- [59] P.-J. Chen, D.C. Rodger, S. Saati, M.S. Humayun, Y.-C. Tai, Microfabricated implantable parylene-based wireless passive intraocular pressure sensors, *Microelectromech. Syst. J.* 17 (2008) 1342–1351.
- [60] G. Mani, M.D. Feldman, D. Patel, C.M. Agrawal, Coronary stents: a materials perspective, *Biomaterials* 28 (2007) 1689–1710.
- [61] B. Lu, S. Zheng, B.Q. Quach, Y.-C. Tai, A study of the autofluorescence of parylene materials for μ TAS applications, *Lab Chip* 10 (2010) 1826–1834.
- [62] E. Meng, P.-Y. Li, Y.-C. Tai, Plasma removal of Parylene C, *J. Micromech. Microeng.* 18 (2008) 045004.
- [63] A.T. Ciftlik, M. Gijs, A low-temperature parylene-to-silicon dioxide bonding technique for high-pressure microfluidics, *J. Micromech. Microeng.* 21 (2011) 035011.
- [64] D.P. Poenar, C. Iliescu, M. Carp, A.J. Pang, K.J. Leck, Glass-based microfluidic device fabricated by parylene wafer-to-wafer bonding for impedance spectroscopy, *Sens. Actuators A Phys.* 139 (2007) 162–171.
- [65] K. Länge, S. Grimm, M. Rapp, Chemical modification of parylene C coatings for SAW biosensors, *Sens. Actuators B Chem.* 125 (2007) 441–446.
- [66] H.L. Jiang, Y.K. Kim, K.H. Cho, Y.C. Jang, Y.J. Choi, J.H. Chung, et al., Roles of spheroid formation of hepatocytes in liver tissue engineering, *Int. J. Stem Cells* 3 (2010) 69–73.
- [67] M.J. Powers, D.M. Janigian, K.E. Wack, C.S. Baker, D. Beer Stolz, L.G. Griffith, Functional behavior of primary rat liver cells in a three-dimensional perfused microarray bioreactor, *Tissue Eng.* 8 (2002) 499–513.
- [68] C. Decaens, M. Durand, B. Grosse, D. Cassio, Which in vitro models could be best used to study hepatocyte polarity? *Biol. Cell.* 100 (2008) 387–398.
- [69] X. Liu, E.L. LeCluyse, K.R. Brouwer, L.S. Gan, J.J. Lemasters, B. Stieger, et al., Biliary excretion in primary rat hepatocytes cultured in a collagen-sandwich configuration, *Am. J. Physiol.* 277 (1999) G12–G21.
- [70] M. Depreter, T. Walker, K. De Smet, S. Beken, I. Kerckaert, V. Rogiers, et al., Hepatocyte polarity and the peroxisomal compartment: a comparative study, *Histochem J.* 34 (2002) 139–151.
- [71] C. Lu, A.P. Li, Species comparison in P450 induction: effects of dexamethasone, omeprazole, and rifampin on P450 isoforms 1A and 3A in primary cultured hepatocytes from man, Sprague–Dawley rat, minipig, and beagle dog, *Chem. Biol. Interact.* 134 (2001) 271–281.
- [72] M. Martignoni, G.M. Groothuis, R. de Kanter, Species differences between mouse, rat, dog, monkey and human CYP-mediated drug metabolism, inhibition and induction, *Expert Opin. Drug Metab. Toxicol.* 2 (2006) 875–894.
- [73] T. Shimada, H. Yamazaki, M. Mimura, Y. Inui, F.P. Guengerich, Interindividual variations in human liver cytochrome P-450 enzymes involved in the oxidation of drugs, carcinogens and toxic chemicals: studies with liver microsomes of 30 Japanese and 30 Caucasians, *J. Pharmacol. Exp. Ther.* 270 (1994) 414–423.
- [74] A. Dash, M.B. Simmers, T.G. Deering, D.J. Berry, R.E. Feaver, N.E. Hastings, et al., Hemodynamic flow improves rat hepatocyte morphology, function, and metabolic activity in vitro, *Am. J. Physiol. Cell Physiol.* 304 (2013) C1053–C1063.